CI&CEQ
Chemical Industry & Chemical Engineering Quarterly

Available online at
Association of the Chemical Engineers of Serbia AChE
www.ache.org.rs/CICEQ

Chem. Ind. Chem. Eng. Q. 29 (4) 273–280 (2023) CI&CEQ

LV CHAO[1,3]
YIN HONGXIN[1]
LIU YANLONG[1]
CHEN XUXIN[1]
SUN MINGHE[1]
ZHAO HONGLIANG[2]

[1]School of Control Engineering, Northeastern University, Hebei, China

[2]School of Metallurgy and Ecological Engineering, University of Science and Technology Beijing, Beijing, China

[3]State Key Laboratory of Complex Nonferrous Metal Resources Clean Utilization, Kunming University of Science and Technology,Yunnan, China

SCIENTIFIC PAPER

UDC 66.092-997:54:519.87

PROCESS STUDY OF CeO_2 PREPARATION BY JET-FLOW PYROLYSIS VIA MICROWAVE HEATING

Article Highlights

- Cerium oxide with high purity was produced via microwave heating
- The effect of gas and material velocity on purity was studied by experiment and numerical simulation
- Single-phase cerium oxide with sphere-like morphology was obtained in this study

Abstract

The spray pyrolysis method has the disadvantage of nozzle plugging, and the conventional heating model causes a large temperature gradient, which leads to unevenly heated reactants. This study used cerium chloride heptahydrate and Venturi reactor as raw material and core equipment. The technology of microwave heating was combined to prepare single-phase sphere-like cerium oxide. The mean size of the particles was near 80nm. The product was characterized via XRD, SEM, and EDS technologies. The purity, morphology, and energy consumption were compared with the conventional spray pyrolysis. Fluent software coupled with HFSS was employed to simulate the effects of different process conditions on products' purity and temperature field in the reactor. There was good correspondence between experimental and simulated results. The results showed that as gas velocity V_g increased, the tendency of the temperature field distribution did not change. The lowest mass fraction of chlorine element reached 0.13% when the gas inlet velocity reached 1.7 m/s. When the material inlet velocity was 0.05 m/s, the mass fraction of the chlorine element was below 0.1%, which indicated that the reactants had a complete reaction. It has been calculated that the heating cost, energy consumption, and CO_2 emission decreased sharply compared with the spray pyrolysis method.

Keywords: cerium oxide, economic benefit, microwave heating, numerical simulation.

Cerium oxide (CeO_2) is the most common composition of rare earth metals with superior characteristics, including high activity, hardness, and stability. Considering the relatively low mining costs of CeO_2, it has been widely applied in numerous fields, such as catalyst, medicine, and abrasive compounds with special physical and chemical properties [1–4].

Studies show that the size and morphology of CeO_2 particles directly affect their physical and chemical properties. In this regard, scholars have utilized different methods, including precipitation [5], gel-sol [6], and pyrolysis, to prepare CeO_2 powder at micro-nano levels. Among these methods, the pyrolysis method has many advantages, like lower cost and higher efficiency. However, it also has the disadvantage of nozzle plugging, which causes frequent replacement, and the experiment cannot be continuously carried out. The roasted products always agglomerated and had varying particle sizes. Aiming at this problem, a method of jet-flow pyrolysis via microwave heating, a new preparation technology of

Correspondence: L. Chao, School of Control Engineering, Northeastern University, Hebei 066004, China.
E-mail: lvchao@neuq.edu.cn
Paper received: 10 May, 2022
Paper revised: 28 November, 2022
Paper accepted: 28 December, 2022

https://doi.org/10.2298/CICEQ220510034C

CeO_2, was developed by our team. This technology has many advantages. For example, the jet effect of the Venturi reactor has been demonstrated to produce an atomization effect on droplets, which perfectly avoided the functional defects of the nozzle [7].

Microwaves are electromagnetic waves with frequencies between 300 MHz and 300 GHz. Based on the penetration characteristic of microwaves, the molecule orientation in the heated object changes with the variation of the microwave field, thereby colliding with nearby molecules and generating heat [8–9]. Microwave heating has the advantages of fast and even heating, which can eliminate the temperature gradient in the reaction system and restrain the products' agglomeration [10–12]. Accordingly, regular morphology and small particle size will be obtained. Due to the opaque equipment, numerical simulation has become an efficient tool to predict and visualize the thermal response of materials subjected to microwave heating [13]. Researchers have conducted numerical simulations to study the interphase transfer process under the microwave field and analyze microwave pyrolysis. Salvi *et al*. [14] simulated the multiphase flow trans-mission and studied the interaction between microwave and fluid by solving Maxwell and heat conduction equations. Then, the effect of temperature distribution and physical properties of the fluid on microwave heating was investigated. Si *et al*. [15] simulated the drying characteristics of lignite in a microwave-fluidized bed based on the Euler model and qualitatively analyzed the heat transfer coefficient, microwave power, and relationship between the gas phase temperature and the gas velocity. In this study, the experiment and simulation were both investigated. It was intended to establish the coupling model of microwave heating, fluid flow, and chemical reaction. Effects of gas and material inlet velocity on temperature field and CeO_2 purity were studied. The heating cost, energy consumption, and CO_2 emission were calculated.

In this study, microwave heating and jet technology are combined to achieve a green and environment-friendly rare earth oxide preparation process with a simple process flow, which aligns with the current low-carbon production concept. At the same time, we use numerical simulation to visually analyze the physical field in the experiment, which provides more reasonable data support for the optimization of the experimental scheme in the future.

MATERIALS AND METHODS

Experiments

The experimental process scheme is shown in Figure 1. Venturi reactor made of quartz was fastened to the center of the microwave oven (Independent design, Shan-Lang Experimental Material Management Department, China). The air compressor (2.0 kW, Jiangsu Dongcheng M&E Tools Co., Ltd, China) provided oxygen for the chemical reaction. The glass rotameter (LZB-15, 1–10 m^3/h, Xiangjin Hardware&Electrical Appliance Co., Ltd) was used to measure the gas velocity generated by the air compressor. The steam generator (LDR3-04, Dongyang Jiaxian Machinery Manufacturing Co., Ltd, China) was used to preheat and provide water vapor for the chemical reaction. Cerium chloride heptahydrate ($CeCl_3·7H_2O$, 99%, analytical grade, Sinopharm Chemical Reagent Co., Ltd, China) was the raw material and entered the Venturi reactor from the vertical material inlet. Driven by the gas, the materials were pushed into the reactor to react with oxygen. The solid product of the reaction fell into the solid-product collector. In the industrial production process of the pyrolysis method, hydrogen chloride (HCl) was used to dissolve rare earth ore or recycle it in the extraction process. However, there were no conditions for HCl recovery in the laboratory. Therefore, the gas produced by the reaction was absorbed by the sodium carbonate (Na_2CO_3, 99.8%, AR, Sinopharm Chemical Reagent Co., Ltd, China) solution.

The phase composition of the products was determined using X-ray diffraction (XRD, Empyrean S3, PANalytical) at a scanning rate of 5°/min in the 2θ range from 10° to 90° with Cu K_α radiation (λ=1.540598 nm).

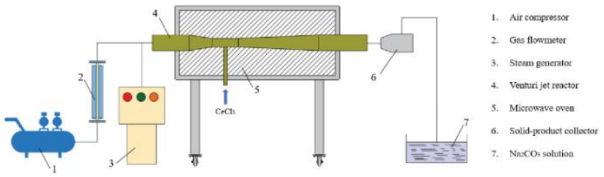

Figure 1. Scheme diagram of the experimental process.

Numerical simulation

The whole numerical simulation was based on the Workbench 19.0 platform. HFSS software was used for the electromagnetic simulation. Fluent software was used to simulate the fluid field and chemical reactions. The two parts were connected using an interface. During numerical simulation, enthalpy, entropy, and other necessities were determined from Practical Inorganic Thermodynamics Data Manual [16].

Geometry

Based on the experimental equipment, the three-dimensional model was simplified and built, as shown in Figure 2. Table 1 presented the sizes of the microwave oven and reactor. The model of the

waveguide was BJ26. The grid of the model consisted of three-dimensional tetrahedral unstructured meshes. In addition, a local coordinate system and an influence sphere were created at the Venturi tube to conduct local encryption on the grid, and the total number of grids reached 370 k.

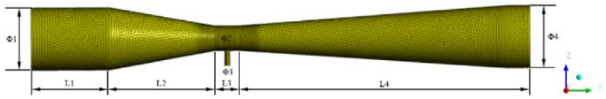

Figure 2. Schematic diagram of Venturi reactor.

Table 1. Mass balance and residence time from thermal cracking products.

	Length (mm)	Width (mm)	Height (mm)	Diameter (mm)
Cavity	690	400	600	-
Waveguide	86.4	43.2	60	-
L1	-	-	100	-
L2	-	-	136	-
L3	-	-	343	-
L4	-	-	30	-
Φ1	-	-	-	30
Φ2	-	-	-	15
Φ3	-	-	-	7
Φ4	-	-	-	30

Four monitoring surfaces were set between the Venturi tube and outlet to study the reactor's temperature field and the content of each substance at each position. The distance between these surfaces and the gas phase inlet was Y_1 = 290 mm, Y_2 = 390 mm, Y_3 = 490 mm, and Y_4 = 590 mm, respectively.

Governing equations

The electromagnetic field distribution of the cavity in the microwave oven, including the reactor, can be determined by solving the Maxwell equation. The time-varying form of the Maxwell equation can be expressed in the form below:

$$\nabla \cdot \boldsymbol{D} = \rho_e \quad (1)$$

$$\nabla \cdot \boldsymbol{B} = 0 \quad (2)$$

$$\nabla \times \boldsymbol{E} = -\frac{\partial \boldsymbol{B}}{\partial t} \quad (3)$$

$$\nabla \times \boldsymbol{H} = -\frac{\partial \boldsymbol{D}}{\partial t} + \boldsymbol{J} \quad (4)$$

where B is the magnetic flux density (Wb/m^3), D is the electric displacement or electric flux density (C/m^2), E is the electric field intensity (V/m), H is the magnetic field intensity (A/m), J is the current density (A/m^2), and ρ_e is the electric charge density (C/m^3).

The complex relative permittivity ε_r is defined as:

$$\varepsilon_r = \varepsilon' + j\varepsilon'' \quad (5)$$

where $j^2 = -1$, ε' is the dielectric constant, and ε'' is the corresponding loss factor (the imaginary part of the dielectric constant). ε' represents the ability of microwaves to penetrate the material, while ε'' represents the ability of the material to store electricity.

The differential wave equation deduced using Maxwell's equations describes the electromagnetic field distribution:

$$\nabla \times \mu_r^{-1}(\nabla \times \boldsymbol{E}) - k_0^2\left(\varepsilon_r - \frac{j\sigma}{\omega\varepsilon_0}\right)\boldsymbol{E} = 0 \quad (6)$$

$$k_0 = \omega / c_0 \quad (7)$$

where ω is the angular frequency (rad/s), ε_0 is the free space permittivity (8.85×10^{-12} F/m), μ_r is the relative permeability, σ represents the electrical conductivity (S/m), k_0 is the wave number in free space, and c_0 represents the speed of light in vacuum (m/s).

When the electromagnetic field interacts with the solution, part of the electromagnetic energy transforms into thermal energy, which is the source item of the energy equation. The energy absorbed by the per unit volume solution can be expressed using the following equation:

$$Q = \frac{1}{2}\omega\varepsilon_0\varepsilon''|\boldsymbol{E}|^2 \quad (8)$$

where $|E|$ is the electric field modulus.

In the reactor, every relative species needs to observe the species mass-conservation equation:

$$\frac{\partial(\rho Y_i)}{\partial t} + \nabla \cdot (\rho \boldsymbol{v} Y_i) = -\nabla \boldsymbol{J}_i + R_i + S_i \quad (9)$$

where Y_i is the mass fraction of the i^{th} substance, R_i is the net production rate of the chemical reaction of the i^{th} substance, S_i is the discrete phase of the i^{th} substance that is responsible for the additional production rate caused by the user-defined source item, and J_i is the diffusive flux of the i^{th} substance produced by the concentration gradient.

The reaction in the Venturi jet pyrolysis reactor is:

$$4CeCl_3(s) + 6H_2O(g) + O_2(g) = 4CeO_2(s) + 12HCl(g) \quad (10)$$

Boundary conditions

The specific boundary conditions are shown in Table 2. The microwave power (P) and frequency (f) were set to 1 kW and 2.45 GHz, respectively. Although there were differences between the real case and the numerical model, the numerical simulation could reveal the effects of experimental factors. Some assumptions were made before the simulation to decrease the difficulty of the simulation and raise its efficiency:

1) The frequency of the microwave is constant at 2.45 GHz.
2) All the fluids in this study are considered incompressible fluids.
3) The initial temperature field is uniform at 300 K (room temperature).

Table 2. Boundary conditions.

	Boundary type	Valve
Excitation	Wave port	-
Wall of waveguides and cavity	Perfect E boundary	-
Gas inlet	Velocity-inlet	1.7 m/s
Material inlet	Velocity-inlet	0.01 m/s
Outlet	Outflow	-

RESULTS AND DISCUSSION

Comparison of experimental results

The XRD pattern of the product is shown in Figure 3. It showed a single phase CeO_2 obtained at the temperature of 901 K. Compared with the spray pyrolysis method at the temperature of 1023 K [17], the intensity of the diffraction peaks was higher. No other impurity peak indicated a better degree of crystallinity and a higher purity of CeO_2. Scanning electron microscope (SEM, Apreo 2C, Thermo scientific) images of nano CeO_2 particles obtained in this study are shown in Figure 4a. Compared with the SEM images of spray pyrolysis shown in Figure 4b, the particles were sphere-like and smaller, so there was less agglomeration. The above indicated that microwave heating could produce purer CeO_2 with more regular morphology at a lower temperature.

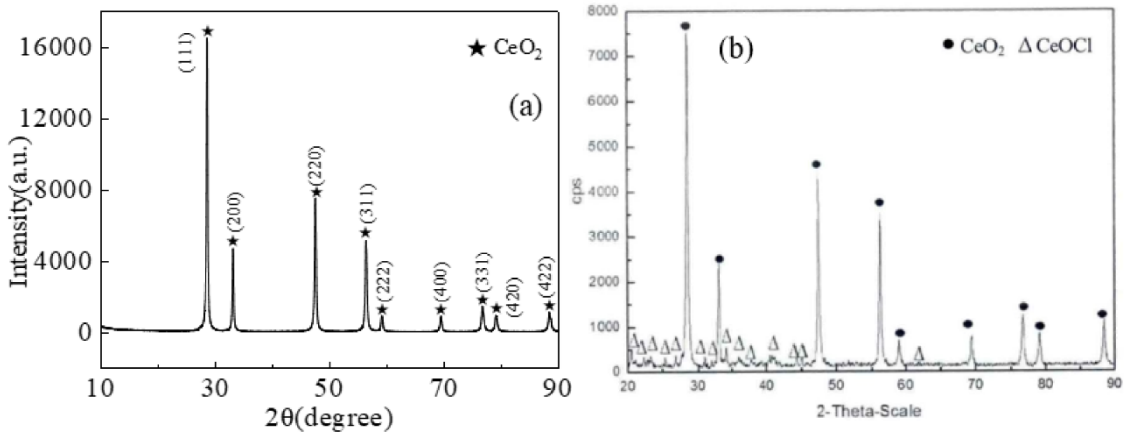

Figure 3. XRD pattern of the product: (a)-this study; and (b)- spray pyrolysis [17].

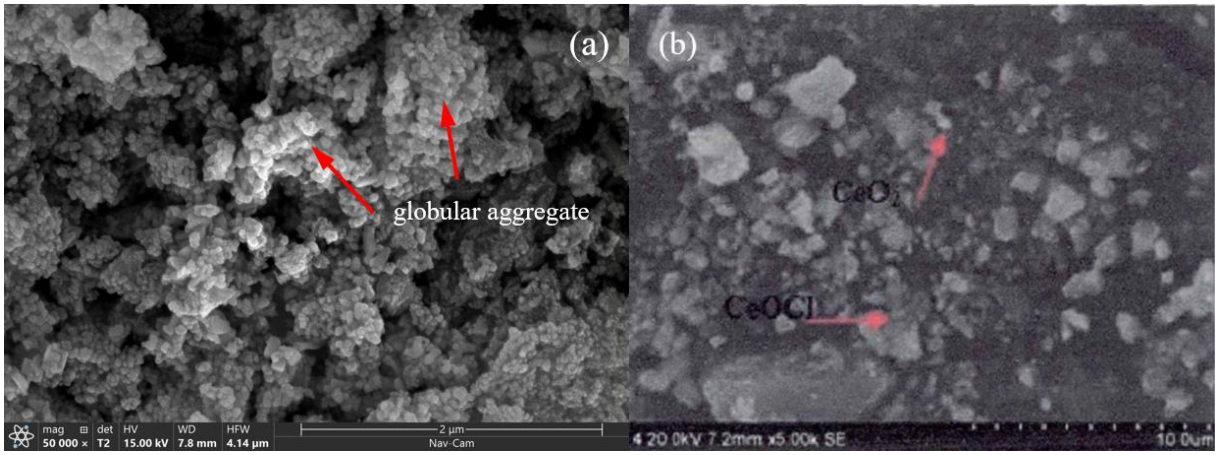

Figure 4. SEM images of the product: (a)-this study; and (b)- spray pyrolysis [17].

Verification

Table 3 presents the comparison of experimental and simulated results. The content of residual chlorine element (M_{Cl}) was used for the evaluation index of the product purity. It was observed that the error between the numerical simulation and experiment was within an acceptable range. Furthermore, it proved that the selected models, measured physical parameters, and

imposed boundary conditions were correct.

Table 3. Model verification.

	Power	Gas velocity	Average temperature	M_{cl}
Experiment	1 kW	2.1 m/s	901 K	1.64%
Simulation	1 kW	2.1 m/s	915.2 K	0.95%
Error	-	-	1.6%	0.7%

Effect of gas phase inlet velocity

Figure 5a illustrates the temperature field in the Venturi reactor. Although it is evident that the central temperature was always higher than the temperature near the wall, it accorded with the characteristics of the microwave heating model. Therefore, this temperature field was the key to obtaining CeO_2 particles with regular morphology and higher purity.

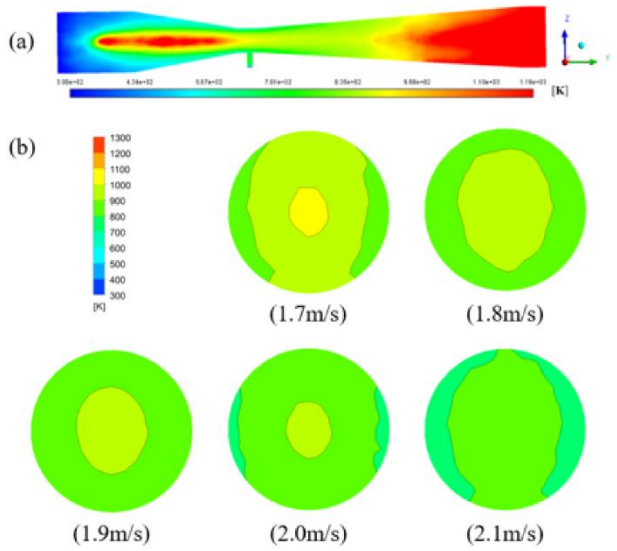

Figure 5. Temperature distribution (a) in the reactor and (b) on Y_2.

Different gas velocity (V_g) was set to 1.7 m/s, 1.8 m/s, 1.9 m/s, 2.0 m/s, and 2.1 m/s, respectively. Figure 5b indicated that the temperature in the reactor was distributed evenly under the microwave field, and there was no dead zone of heat and little temperature gradient. When V_g = 1.7 m/s, the center temperature of the monitoring surface exceeded 1000 K. When V_g = 1.8 ~ 2.1 m/s, the center temperature was lower than 1000 K, and the highest center temperature area decreased gradually. The increase of V_g decreased the reactor temperature, but it had a negligible impact on the tendency of temperature distribution. Figure 6a showed that the increase of gas inlet velocity increased the local velocity at the Venturi tube, the gas and raw material had a better mixing, but the heating time of $CeCl_3$ was shortened. The mass fraction of CeO_2 reached 99.7% when V_g = 1.7 m/s, which indicated that the highest reaction involvement of raw material was achieved. With gas velocity increasing, chlorine element content increased on each monitoring surface. It indicated that increasing gas velocity decreased the purity of CeO_2, as shown in Figure 6b.

Effect of raw material inlet velocity

When V_g=2.1 m/s, the effect of various material inlet velocities (0.01 m/s, 0.02 m/s, 0.03 m/s, 0.04 m/s, and 0.05 m/s) on the purity of CeO_2 was investigated. The nephogram of the CeO_2 mass fraction at the outlet is shown in Figure 7a.

The effect of material velocity (V_m) on the reaction is shown in Figure 7b. It was observed that when V_m = 0.01 m/s, the purity of CeO_2 was lower than 98%. Under this circumstance, the insufficient initial velocity of $CeCl_3$ prevented it from increasing to a higher height to mix with the oxygen. Subsequently, $CeCl_3$ deposited at the bottom, causing an incomplete reaction. When V_m = 0.02 m/s, CeO_2 purity increased by 1%. When V_m = 0.05 m/s, CeO_2 purity reached 99.8%, indicating that $CeCl_3$ mixed well with oxygen

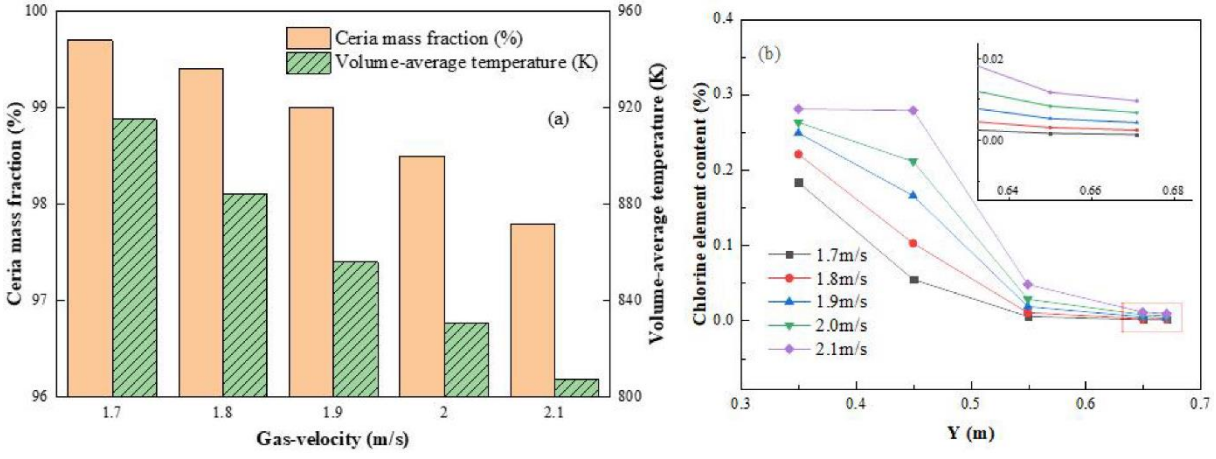

Figure 6. (a) Effect of the gas inlet velocity on Cerium oxide mass faction and volume-average temperature; and (b) Chlorine element content on each monitoring surface.

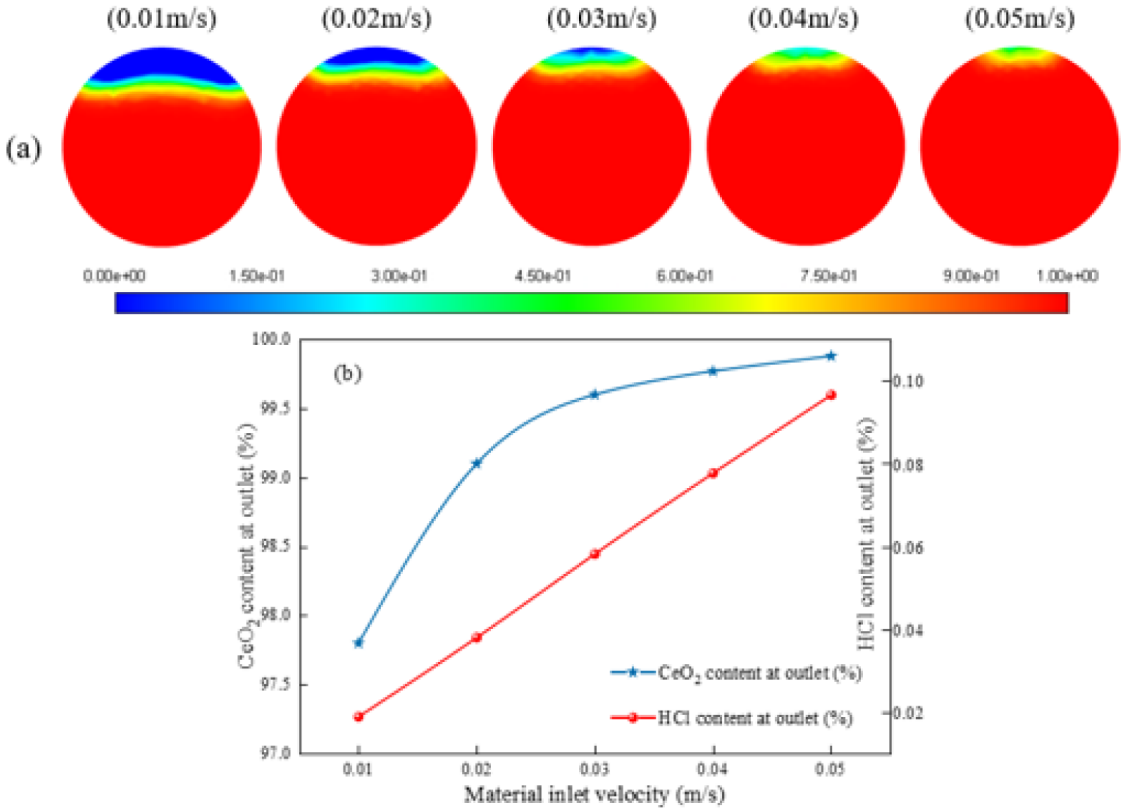

Figure 7. (a) Nephogram of CeO_2 content at the outlet; and (b) Effect of the gas phase inlet velocity on CeO_2 content at the outlet.

by this condition. On the other hand, the content of HCl continuously increased as the material velocity increased. Therefore, it proved that increasing material velocity benefited the chemical reaction. Among the five studied cases, the best results were achieved when V_m = 0.05 m/s.

Energy consumption and cost calculation

According to the experimental process of spray pyrolysis, the heating cost, energy consumption, and carbon dioxide (CO_2) emission were calculated under microwave jet-flow pyrolysis and spray pyrolysis using Eqs (11–16). The CO_2 emission calculation in this study was based on the CO_2 produced by the coal-fired electric generation according to the electric quantity used by the microwave oven. However, there was no CO_2 emission during the whole experimental process. As a result, the heating cost, energy consumption, and CO_2 emission were sharply decreased, as shown in Figure 8. It indicated that microwave jet-flow pyrolysis not only had the advantages of improving particles' morphology but also had a better economic benefit and lower carbon emission than spray pyrolysis. Furthermore, the costs will be further reduced if the production reaches an industrial scale.

$$C_1 = V\rho p_1 \tag{11}$$

where C_1 is the heating cost of spray pyrolysis (yuan) when 27 g CeO_2 is prepared, V is the volume consumption of propane, 24.7 (m^3), ρ is the density of propane 1.83 (kg/m^3), P_1 is the price of propane, 4.9 (yuan/kg).

$$C_2 = 27P_{micro}p_2/Q\varphi \tag{12}$$

where C_2 is the cost of microwave heating (yuan) when 27 g CeO_2 is prepared, P_{micro} is microwave power, 1 (kW), φ is the efficiency of a microwave oven, which is 70%, p_2 is the industrial electric charge, 1.5 (yuan/kWh), Q is the mass flow rate of CeO_2 at the outlet of the reactor 28.044 (g/h).

$$E_1 = b_1V \tag{13}$$

where E_1 is the energy consumption of spray pyrolysis method (kJ), b_1 is the burn value of propane, which is 1.0152e+5 (kJ/m^3), V is the volume consumption of propane, 24.7 (m^3).

$$E_2 = 3.6*10^6*27P_{micro}/Q\varphi \tag{14}$$

where E_2 is the energy consumption of microwave heating (kJ).

$$e_1 = 3VpM_{co_2}/M_{pro} \tag{15}$$

where e_1 is CO_2 emission of spray pyrolysis method (kg), M_{co_2} represents the molecular weight of CO_2, which is 44. M_{pro} represents the molecular weight of propane, which is 44.1.

$$e_2 = 27fP_{micro}/Q\varphi \quad (16)$$

where e_2 is the CO_2 emission of thermal power (kg), and f represents the CO_2 emission per kilowatt-hour generation, 0.785 (kg/kWh).

CONCLUSION

According to the XRD pattern, a single-phase CeO_2 was obtained, and the crystal grew well. SEM images showed CeO_2 nanoparticles obtained in this study had sphere-like morphology and smaller size. The increase of the gas inlet velocity decreased the average temperature when V_g = 1.7 m/s, V_m = 0.05 m/s, and the mass fraction of CeO_2 at the outlet reached 99.7% and 99.8%, respectively. Compared with the spray pyrolysis method, the heating cost, energy consumption, and CO_2 emission were sharply decreased in this study. Furthermore, it demonstrated that jet-flow pyrolysis via microwave heating was a low-carbon and cost technology.

ACKNOWLEDGEMENTS

This research was supported by the National Natural Science Foundation of China(51904069), the Fundamental Research Funds for the Central Universities(N2223026), and the Scientific Research Fund Project of Northeastern University at Qinhuangdao (XNY201808).

REFERENCES

[1] K.B. Kusuma, M. Manju, C.R. Ravikumar, N. Raghavendra, M.A. Shilpa Amulya, H.P. Nagaswarupa, H.C. Ananda Murthy, M.R. Anil Kumar, T.R. Shashi Shekhar, Appl. Surf. Sci. Adv. 11 (2022) 100304. https://doi.org/10.1016/j.apsadv.2022.100304.

[2] P. Janos, J. Ederer, V. Pilarova, J. Henych, J. Tolasz, D. Milde, T. Opletal, Wear 362-363 (2016) 114–120. https://doi.org/10.1016/j.wear.2016.05.020.

[3] S.J. Liang, X. Jiao, X.H. Tan, J.Q. Zhu, Appl. Opt. 57 (2018) 5657–5665. https://doi.org/10.1364/AO.57.005657.

[4] F. Wei, C.J. Neal, T.S. Sakthivel, Y.F. Yu, M. Omer, A. Adhikary, S. Ward, K.M. Ta, Bioact. Mater. 21 (2023) 547–565. https://doi.org/10.1016/j.bioactmat.2022.09.011.

[5] M. Ramachandran, M. Shanthi, R. Subadevi, M. Sivakumar, Vacuum 161 (2019) 220–224. https://doi.org/10.1016/j.vacuum.2018.12.002.

[6] S. Gnanam, V. Rajendran, J. Alloys Compd. 735 (2018) 1854–1862. https://doi.org/10.1016/j.jallcom.2017.11.330.

[7] C. Lv, Q.Y. Zhao, Z.M. Zhang, Z.H. Dou, T.A. Zhang, H.L. Zhao, Trans. Nonferrous Met. Soc. China 25 (2015) 997–1003. https://doi.org/10.1016/S1003-6326(15)63690-1.

[8] A.Z. Fia, J. Amorim, Energy 218 (2021) 119472. https://doi.org/10.1016/j.energy.2020.119472.

[9] J. Liu, J.H. Liu, B.W. Wu, S.B. Shen, G.H. Yuan, L.Z. Peng, Chin. J. Eng. 39 (2017) 208–214. DOI: 10.13374/j.issn2095-9389.2017.02.007.

[10] E. Meloni, M. Martino, M. Pierro, P. Pullumbi, F. Brandani, V. Palma, Energies 15 (2022) 4119. https://doi.org/10.3390/en15114119.

[11] V. Palam, D. Barba, M. Cortese, M. Martino, S. Renda, E. Meloni, Catalysts 10 (2020) 246. https://doi.org/10.3390/catal10020246.

[12] E. Meloni, M. Martino, V. Palma, Renewable Energy 197 (2022) 893–931. https://doi.org/10.1016/j.renene.2022.07.157.

[13] J.Y. Zhu, L.P. Yi, Z.Z. Yang, M. Duan, Chem. Eng. J. 407 (2021) 127197. https://doi.org/10.1016/j.cej.2020.127197.

[14] D. Salvi, D. Boldor, G.M. Aita, C.M. Sabliov, J. Food Eng. 104 (2011) 422429. https://doi.org/10.1016/j.jfoodeng.2011.01.005.

[15] C.D. Si, J.J. Wu, Y.X. Zhang, G.J. Liu, Q.J. Guo, Fuel 242 (2019) 159–149. https://doi.org/10.1016/j.fuel.2019.01.002.

[16] D.L. Ye. Practical Inorganic Thermodynamics Data Manual; Cao, S.L., Ed., Metallurgical Industry Press, Beijing (1981), p. 262–263, 265-266. ISBN:7-5024-3055-5.

[17] X.H. Liu. (2011). [Master's Thesis, Northeastern University]. China National Knowledge Infrastructure. https://kns.cnki.net/kcms2/article/abstract?v=3uoqIhG8C475KOm_zrgu4lQARvep2SAkbI4wwVeJ9RmnJRGnwiiNVgbPSHgq3mML_3baomtbo8MY72vRZI789SFqng4qPhOf&uniplatform=NZKPT.

LV CHAO[1,3]
YIN HONGXIN[1]
LIU YANLONG[1]
CHEN XUXIN[1]
SUN MINGHE[1]
ZHAO HONGLIANG[2]

[1]School of Control Engineering, Northeastern University, Hebei, China

[2]School of Metallurgy and Ecological Engineering, University of Science and Technology Beijing, Beijing, China

[3]State Key Laboratory of Complex Nonferrous Metal Resources Clean Utilization, Kunming University of Science and Technology,Yunnan, China

NAUČNI RAD

PROUČAVANJE PROCESA PRIPREME CeO_2 PIROLIZOM U VENTURI REAKTORU SA MIKROTALASNIM ZAGREVANJEM

Metoda pirolize raspršivanjem ima nedostatak začepljenja mlaznica, a konvencionalni model grejanja izaziva veliki temperaturni gradijent, što dovodi do neravnomernog grejanja reaktanata. U ovom korišćeni su cerijum-hlorid heptahidrat i Venturi reaktor. Mikrotalasno zagrevanja je korišćeno da bi se pripremio jednofazni sferični cerijum oksid. Srednja veličina čestica bila je blizu 80 nm. Proizvod je okarakterisan XRD, SEM i EDS tehnikama. Čistoća, morfologija i potrošnja energije su upoređeni sa konvencionalnom pirolizom raspršivanjem. Softver Fluent, u kombinaciji sa HFSS, korišćen je za simulaciju efekata različitih uslova procesa na čistoću proizvoda i temperaturno polje u reaktoru. Utvrđeno je dobro slaganje između eksperimentalnih i simuliranih rezultata. Rezultati su pokazali da se sa povećanjem brzine gasa distribucija temperaturnog polja ne menja. Najmanji maseni udeo elementa hlora od 0,13% postignut je kada je brzina ulaznog gasa bila 1,7 m/s. Kada je ulazna brzina materijala bila 0,05 m/s, maseni udeo elementa hlora je bio ispod 0,1%, što je ukazivalo na potpunu reakciju reaktanata. Izračunato je da su troškovi grejanja, potrošnja energije i emisija CO_2 naglo smanjeni u poređenju sa metodom pirolize raspršivanjem.

Ključne reči: cerijum oksid, ekonomska korist, mikrotalasno zagrevanje, numerička simulacija.